

Supporting Information

for

Crystallization Mechanism of a Family of Embedded Isoreticular Zeolites

Jung Gi Min, Hyun June Choi, Jiho Shin, and Suk Bong Hong*

Center for Ordered Nanoporous Materials Synthesis, Division of Environmental Science and
Engineering, POSTECH, Pohang 37673, Korea

Table S1. Numbers of Seven Different Types of Cages in the Unit of ECR-18, ZSM-25, and PST-20

	 [4 ¹² 6 ⁸ 8 ⁶] <i>lta</i>	 [4 ⁸ 8 ²] <i>d8r</i>	 [4 ¹² 8 ⁶] <i>pau</i>	 [4 ⁶ 6 ² 8 ⁶] <i>t-plg</i>	 [4 ⁵ 8 ³] <i>t-oto</i>	 [4 ⁶ 8 ⁴] <i>t-gsm</i>	 [4 ⁷ 8 ⁵] <i>t-phi</i>
ECR-18 (RHO-G3)	2	18	12	16	72	12	24
ZSM-25 (RHO-G4)	2	24	18	24	144	60	72
PST-20 (RHO-G5)	2	30	24	32	240	168	144

Table S2. Oxide Compositions of the TEA⁺-Containing Aluminosilicate Gels Used for the Synthesis of ECR-18, ZSM-25, and PST-20

target zeolite	gel composition	crystallization temperature, K	seed crystals used
ECR-18	1.4TEA ₂ O·0.9Na ₂ O·0.4K ₂ O·1.0Al ₂ O ₃ ·9.0SiO ₂ ·140H ₂ O	373	none
ZSM-25	2.6TEA ₂ O·1.9Na ₂ O·1.0Al ₂ O ₃ ·7.2SiO ₂ ·390H ₂ O	408	none
PST-20	2.6TEA ₂ O·1.9Na ₂ O·0.25SrO·1.0Al ₂ O ₃ ·7.2SiO ₂ ·390H ₂ O	418	PST-20 ^a

^aA small amount (2 wt% of anhydrous raw materials) of as-made PST-20 crystals, which were previously synthesized according to the procedure given in ref. 8, was added as seeds to the synthesis mixture.

Table S3. Chemical Composition Data for a Series of Solid Products of Recovered after Heating under Rotation (60 rpm) at 373, 408, and 418 K for Various Times during the Synthesis of ECR-18, ZSM-25, and PST-20, Respectively

time (h)	%N	%C	%H	ΣCHN^a	%Na ⁺	%K ⁺	%Sr ²⁺	%Si	%Al	Si/Al	Na ⁺ /Al	K ⁺ /Al	Sr ²⁺ /Al	TEA ⁺ /Al	T_{\max} (°C) ^b
ECR-18 synthesis															
0	0.06	0.55	1.10	1.70 (1.8)	2.81	2.92	-	33.39	5.18	6.19	0.64	0.39	-	0.07	340
54	0.18	1.21	1.67	3.05 (3.3)	4.12	4.34	-	26.71	7.89	3.25	0.61	0.38	-	0.08	420
108	0.17	1.04	1.63	2.83 (3.6)	4.13	4.50	-	26.54	7.87	3.24	0.62	0.39	-	0.07	460
110	0.34	1.95	1.85	4.14 (4.3)	3.71	4.31	-	26.54	7.40	3.45	0.59	0.40	-	0.12	470
116	0.36	2.31	2.00	4.67 (4.6)	3.64	4.37	-	26.75	7.57	3.39	0.56	0.40	-	0.13	470
122 ^c	0.48	3.13	2.15	5.76 (5.9)	3.20	4.32	-	26.24	7.22	3.49	0.52	0.41	-	0.17	470
ZSM-25 synthesis															
0	0.07	0.34	0.41	0.82 (1.1)	0.99	-	-	38.74	2.25	16.54	0.85	-	-	0.08	355
40	0.28	1.06	1.75	3.09 (3.5)	6.96	-	-	28.23	8.46	3.21	0.97	-	-	0.08	430
81	0.33	1.10	1.76	3.19 (4.3)	6.95	-	-	27.89	8.10	3.31	1.01	-	-	0.08	440
86	0.48	1.65	2.00	4.13 (4.5)	6.37	-	-	27.42	8.02	3.28	0.93	-	-	0.11	450
96 ^c	0.59	2.49	2.16	5.24 (4.6)	5.98	-	-	27.09	7.79	3.43	0.90	-	-	0.14	450
106	0.57	2.41	2.19	5.17 (5.0)	5.95	-	-	26.87	7.70	3.35	0.91	-	-	0.14	450
PST-20 synthesis															
0	0.10	0.21	0.74	0.76 (2.1)	0.10	-	1.88	40.27	1.03	37.55	0.11	-	0.56	0.15	360
20	0.14	0.81	1.63	2.57 (2.7)	2.68	-	6.92	27.06	7.32	3.55	0.43	-	0.29	0.07	450
30	0.15	0.85	1.70	2.71 (3.0)	2.41	-	6.79	26.99	7.35	3.53	0.38	-	0.28	0.08	450
38.3	0.20	1.23	2.34	3.77 (3.8)	2.23	-	6.51	26.52	7.45	3.42	0.35	-	0.27	0.10	460
38.7	0.20	1.49	2.09	3.78 (4.3)	1.72	-	6.20	26.02	7.47	3.35	0.28	-	0.26	0.10	470
72 ^c	0.51	2.17	2.16	4.97 (4.8)	1.53	-	5.65	26.07	7.49	3.33	0.24	-	0.23	0.13	470

^aTotal organic content in wt%. Values in parentheses are exothermic weight losses determined by TGA/DTA at 523 -823 K. ^bTemperature of the exothermic peak maximum in DTA. ^cFrom a combination of elemental and thermal analyses, these samples, considered as fully crystallized here, were determined to have the unit cell compositions $[(\text{N}(\text{C}_2\text{H}_5)_4)_{26}\text{Na}_{78}\text{K}_{62}(\text{OH})_{16}(\text{H}_2\text{O})_{650}][\text{Al}_{150}\text{Si}_{522}\text{O}_{1344}]$ (ECR-18), $[(\text{N}(\text{C}_2\text{H}_5)_4)_{45}\text{Na}_{292}(\text{OH})_{12}(\text{H}_2\text{O})_{600}][\text{Al}_{325}\text{Si}_{1115}\text{O}_{2880}]$ (ZSM-25), and $[(\text{N}(\text{C}_2\text{H}_5)_4)_{79}\text{Na}_{145}\text{Sr}_{141}\text{H}_{102}(\text{H}_2\text{O})_{1200}][\text{Al}_{608}\text{Si}_{2032}\text{O}_{5280}]$ (PST-20), respectively. H⁺ or OH⁻ was introduced to make each zeolite electrically neutral.

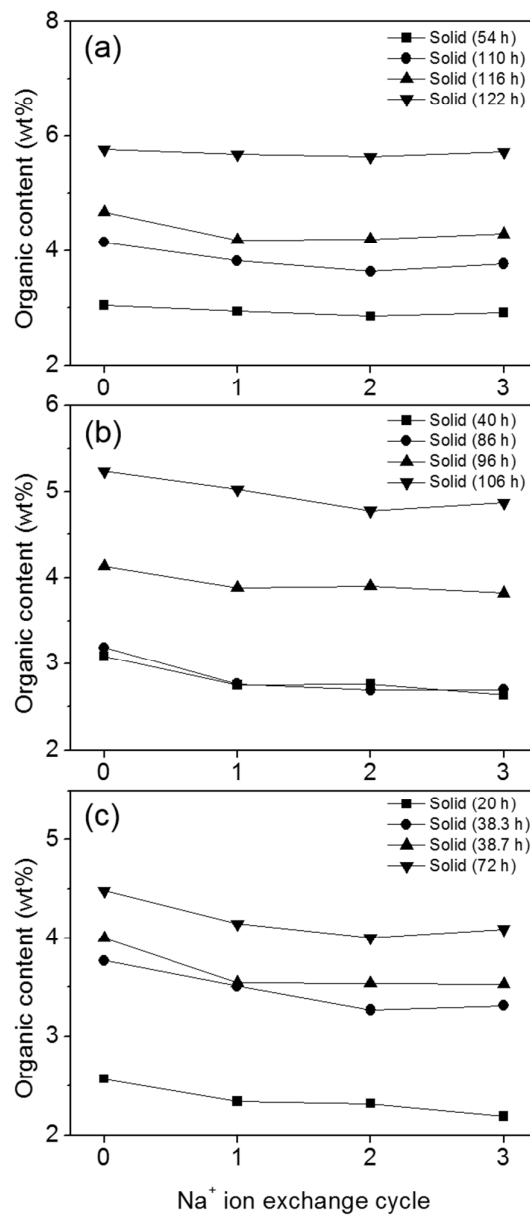


Figure S1. Changes in the organic content (the exothermic weight loss determined by TGA/DTA at 523 – 823 K) of some solid products separated after crystallization of (a) ECR-18, (b) ZSM-25, and (c) PST-20 under rotation (60 rpm) at 373, 408, and 418 K for different times, respectively, followed by repeated ion exchange in 1.0 M NaNO_3 solutions at 353 K for 4 h.

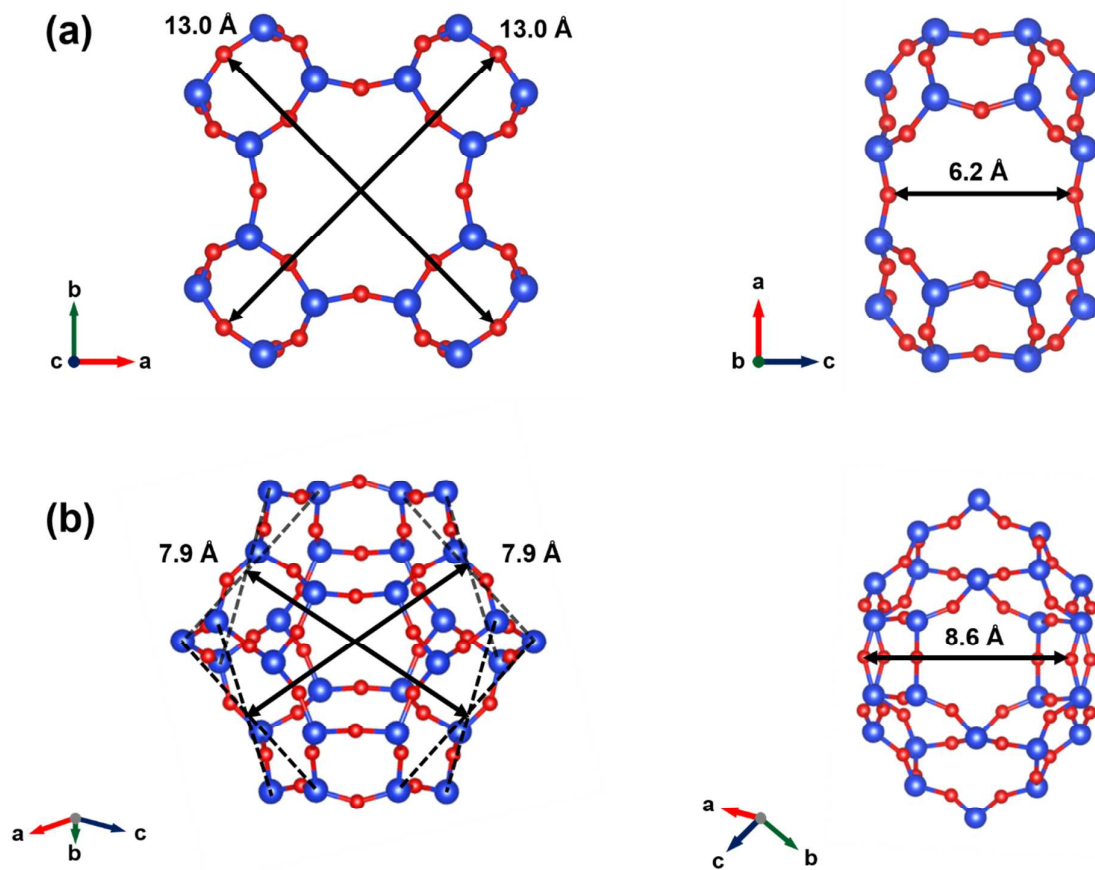


Figure S2. Crystallographic dimensions of (a) *pau* and (b) *t-plg* cages in the RHO-family of embedded isoreticular zeolites.

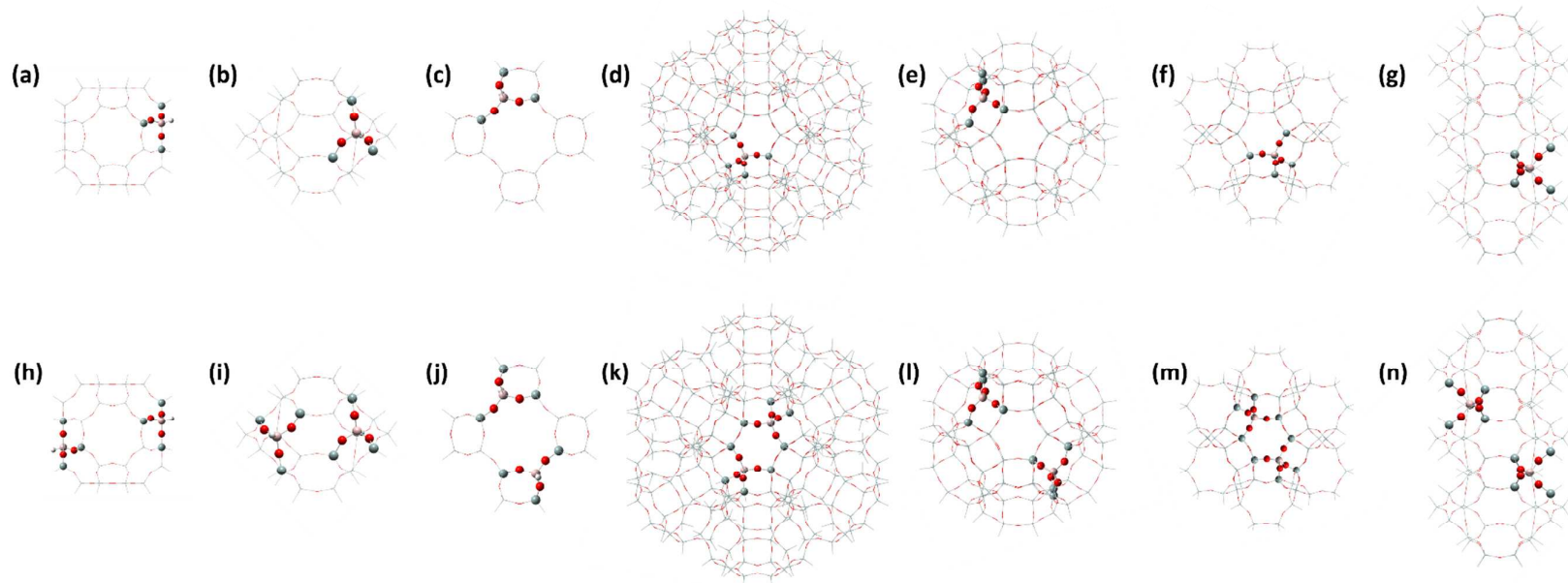


Figure S3. Illustrations of (left to right) discrete *lta*, *t-plg*, *pau* cages and cluster models 1 *lta* cage + 8 *t-plg* cages, 1 *lta* cage + 6 *d8r* cages, 1 *t-plg* cage + 4 *t-oto* cages, and 3 *t-plg* cages with (a) – (g) one; (h) – (n) two framework Al atoms of the RHO family zeolite structure employed in the quantum-chemical calculations on the stabilization energies for various combinations of Na^+ , TEA^+ , and hydrated Na^+ (i.e., an octahedral $[\text{Na}(\text{H}_2\text{O})_6]^+$ complex). Al, pink; Si, Grey; O, red. The 5T cluster active center $[\text{Al}(\text{SiO})_4]$ and located cations were treated at the high M06-2X level, whereas the rest of the tetrahedral atoms (T-atoms) fixed at their crystallographic locations were treated at the low MNDO level.